Subcellular IR Spectromicroscopy

DOI: 10.1002/anie.201003161

Subcellular IR Imaging of a Metal–Carbonyl Moiety Using Photothermally Induced Resonance**

Clotilde Policar, Jenny Birgitta Waern, Marie-Aude Plamont, Sylvain Clède, Céline Mayet, Rui Prazeres, Jean-Michel Ortega, Anne Vessières, and Alexandre Dazzi*

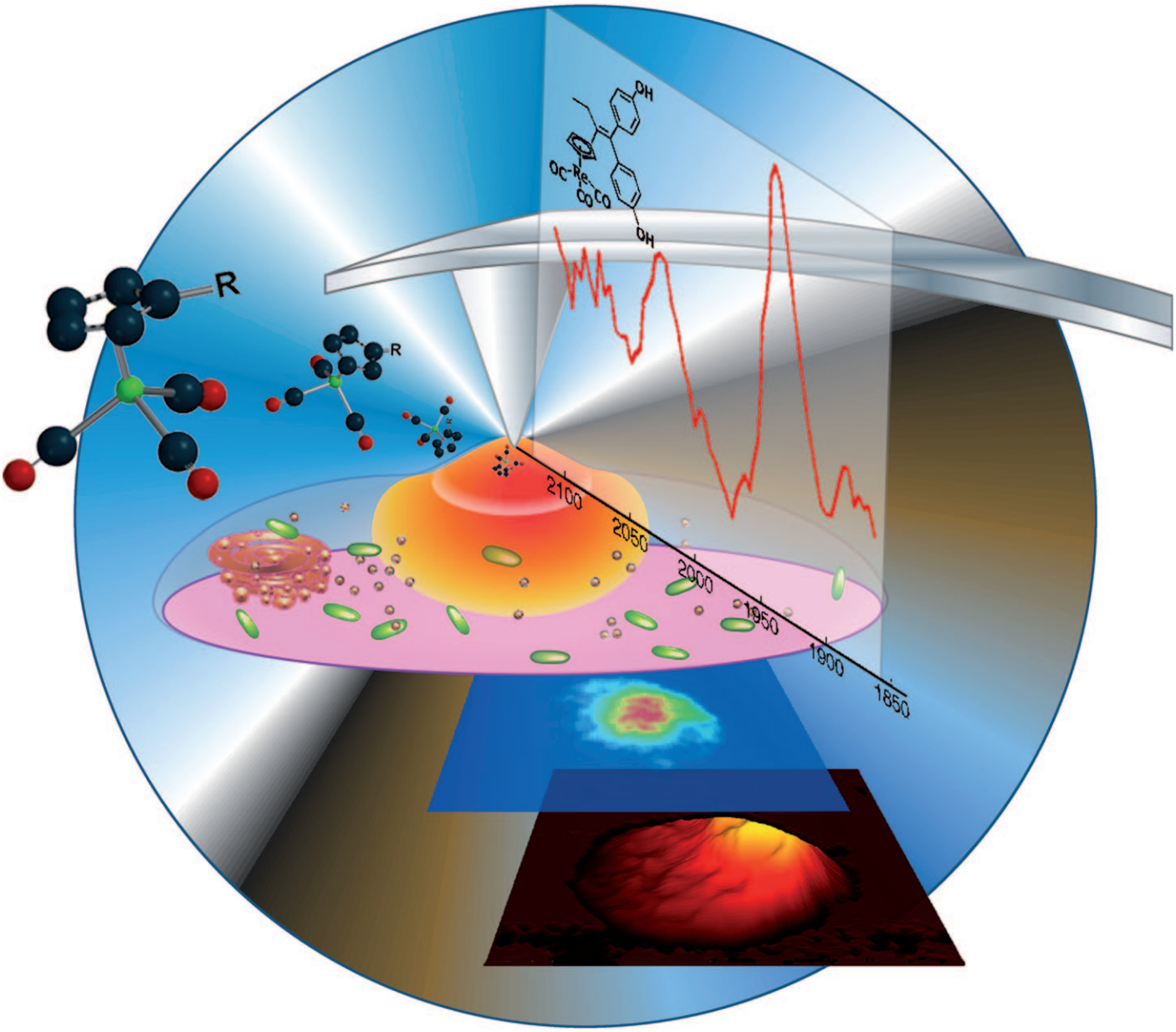

The most widely developed techniques for bio-imaging are those based on fluorescence spectroscopy. However, vibrational spectroscopic techniques, including infrared (IR), Raman, and CARS (coherent anti-Stokes Raman scattering), are also valuable for bioimaging, and they are already in use for the topological analysis of tissues.[1,2] The IR probes described in the literature, generally metal–carbonyl compounds, show many advantages including stability in biological environments and intense absorption in the 1800–2200 cm^{-1} region where biological samples are transparent. Thanks to their specific IR signals, it is possible to detect submicromolar concentrations of these probes quantitatively.[3] Metal–carbonyl compounds have been used as labels,[4–6] for immunoassays,[7–9] and as local pH probes[7] and in a few cases for cellular mapping, but always with spatial resolution above several micrometers using FTIR[10] or Raman microspectroscopy.[11,12] In the case of vibrational excitation in the IR, no photobleaching is induced, in contrast to what is observed with organic fluorophores in the visible or UV range. Moreover, IR tags are of small size, a further reason why they are attractive.[5,7,8] However in classical optical microscopy, submicrometric resolution is not attainable in the IR range as the diffraction criterium imposes resolution higher than $\lambda/2$ (i.e. 2.5 μm at $\lambda = 2000\ cm^{-1}$);[13] this is not suitable for intracellular mapping. But submicrometric resolution is possible using near-field techniques.[14,15]

Photothermally induced resonance (PTIR) is a cutting-edge near-field technique using a setup patented by Dazzi et al.,[16] in which an atomic force microscope (AFM) is coupled with a tunable pulsed infrared laser[17] to record spatially resolved absorption measurements.[18–21] The AFM tip is in contact with the sample (here a cell) which is illuminated by a pulsed laser beam passed through a ZnSe prism (see Figure 1 a).[22] The laser wavelength (λ) is tuned to an IR absorption band of a molecule and, when the laser pulse occurs (see Figure 1 b), the temperature increases locally with local temporary deformations. The AFM tip detects these local deformations and starts to oscillate (see Figure 1 c). The maximum amplitude of this oscillation, which corresponds to the PTIR signal, is proportional to the local absorbance $A(\lambda)$.[15] The resolution of this technique is that of the AFM (ca. 20–50 nm),[15,23] thus allowing the subcellular IR mapping of biological samples. For example, Dazzi et al. have successfully mapped a single air-dried *E. coli* cell by irradiation in the amide I and II wavelength bands (proteins)[18] and have also located DNA from a virus inside *E. coli* by irradiation in the phosphate symmetric band.[19] In both cases, the molecules under investigation were endogenous concentrated cellular components (proteins, DNA). The next challenge for this technique is the identification and localization of exogenous diluted compounds inside cells.

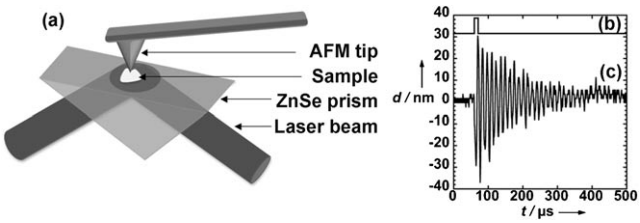

Figure 1. a) Schematic view of the PTIR setup showing the ZnSe prism and the cantilever of the AFM probing the sample. b) Laser pulse. c) Oscillations and relaxation of the AFM cantilever; the temporary thermal deformations of the sample are detected as excitement of the eigenmodes of the AFM cantilever, which relaxes in a few hundred microseconds (d = deflection of the tip).[17,22]

The organometallic conjugate **1**, in which a $[(Cp)Re(CO)_3]$ unit is linked to a hydroxytamoxifen-like structure (Figure 2),[24] is robust in biological media and shows intense CO bands; it has been selected to study cellular uptake and distribution in breast cancer cells (MDA-MB-231) using both transmission-IR spectroscopy for quantification and PTIR spectroscopy for localization and imaging. Organometallic compounds such as **1** are known to be lipophilic,[25,26] thus ensuring good intracellular penetration.[24] In addition, **1** has been described to interact with estrogen receptors, thus inducing the proliferation of hormone-dependent breast cancer cells.[24]

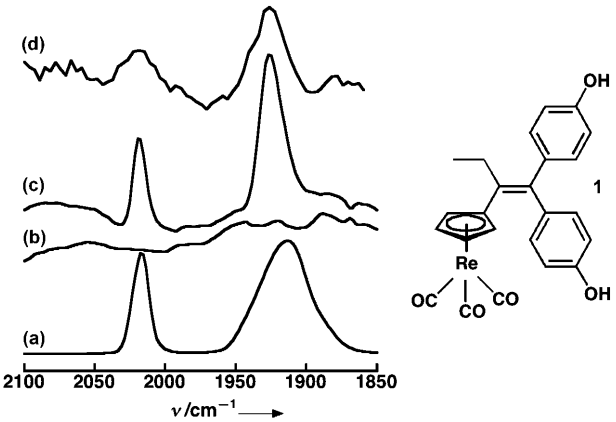

Figure 2. a) FTIR spectrum of pure **1**; b) FTIR spectrum of control cells; c) FTIR spectrum of cells treated with **1** at a concentration 50 μM; d) PTIR spectrum at the nucleus for a single cell treated with **1** (1 h, incubation concentration: 10 μM), average incident power of the laser: 30 mW (see text for details).

[*] Prof. Dr. C. Policar, S. Clède
Laboratoire des BioMolécules, Université Paris 6
CNRS-UMR7203, Département Chimie de l'ENS
24 rue Lhomond 75231 Paris Cedex 05 (France)
Fax: (+33) 1-4432-3389
E-mail: clotilde.policar@ens.fr
Dr. J. B. Waern
ICMMO, Université Paris-Sud 11, CNRS-UMR8182
91405 Orsay Cedex (France)
M.-A. Plamont, Dr. A. Vessières
Laboratoire Charles Friedel, UMR7223, ENSCP
11, rue Pierre et Marie Curie, 75231 Paris Cedex 05 (France)
C. Mayet, Dr. R. Prazeres, Dr. J.-M. Ortega, Dr. A. Dazzi
LCP, Université Paris-Sud 11, CNRS-UMR8000
91405 Orsay Cedex (France)

[**] We thank Prof. Dr. G. Jaouen for helpful discussions and Dr. P. Pigeon for the gift of complex **1**. PIR-CNRS-PCV-prise de risque is also gratefully acknowledged for financial support and the CLIO scientific committee for beam-line time on the AFMIR experiment.
Supporting information for this article is available on the WWW under http://dx.doi.org/10.1002/anie.201003161.

Compound **1** displays two bands in the 2200–1800 cm^{-1} region characteristic of metal-tricarbonyl compounds[3,7] at 1915 cm^{-1} ($\nu_{antisym}$, e) and at 2017 cm^{-1} (ν_{sym}, a_1) (Figure 2a). The cells were incubated for 1 hour with solutions of **1** at concentrations in the micromolar range typically used for such biological studies (5 μM, 10 μM, and 50 μM).[24] After treatment (see the Supporting Information), a known number of cells were deposited on a nitrocellulose disk, which is IR-transparent in the region 1800–2500 cm^{-1}. Very clear signals corresponding to compound **1**, with a slight shift of the $\nu_{antisym}$ band to 1925 cm^{-1},[7] were observed in the classical transmission FTIR spectrum (Figure 2c), indicating that **1** is present in the cells (for comparison see Figure 2b for the FTIR spectrum of the control cells).

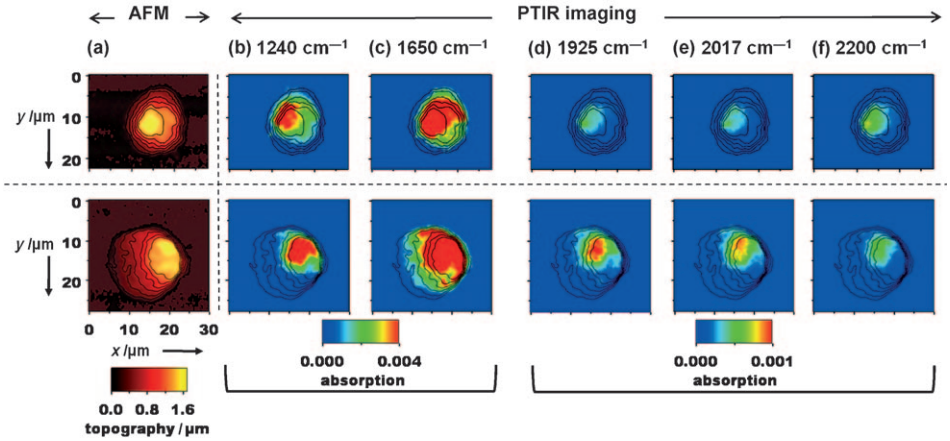

Figure 3. Images of MDA-MB-231 cells. Top row: control cells; bottom row: cells treated with a 10 μM solution of **1** for 1 h at 37 °C. a) AFM topography; b–f) PTIR mappings at different wavelengths, with the AFM contours superimposed as black lines; the wavelengths correspond to the following bands: phosphate (b), amide (c), tricarbonyl (d and e), and out of band (f).

Using a calibration curve generated for **1** (see Figure S1 in the Supporting Information), we quantified the amount of **1** in the cells. The signal at 2017 cm^{-1} was used[3] as it is a unique narrow ν_{sym} IR band, while the signal at 1925 cm^{-1} corresponds to an envelope of two bands, with possible slight shifts.[7] The results obtained for three incubations (5 μM, 10 μM, and 50 μM) investigated in two separate experiments are shown in Table 1 (see also Figures S2 and S3 in the Supporting Information). In the range tested, the amount of **1** in the cells increases with the incubation concentration, which indicates that uptake of **1** is not saturated even at 50 μM.

Table 1: Quantification of the amount content of **1** in a collection of cells (ca. 50000 cells) by FTIR spectroscopy.[a]

Incubation concentration [μM]	Amount of **1** [mole per cell]
5	$(3.1\pm0.2)\times10^{-15}$
10	$(4.8\pm0.2)\times10^{-15}$
50	$(18\pm1.8)\times10^{-15}$

[a] Determined from four measurements (see the Supporting Infroamtion for details).

To map the distribution of **1** inside the cells using PTIR, they were incubated with a 10 μM solution of **1** for 1 hour, then washed and deposited on a ZnSe prism; control cells were processed in a similar way (see the Supporting Information for details). The cells were initially located using the AFM methods (see topography in color and black contours showing the AFM topography in Figures 3 and 4) and were then mapped using the PTIR setup at several wavelengths. Figure 3 presents a series of images both for a control cell and a treated cell.

We will first focus on the images recorded upon irradiation at 1925 cm^{-1} and 2017 cm^{-1} (IR bands of **1**) and at 2200 cm^{-1} (out of band). The control cell shows a weak PTIR signal at these three frequencies (Figure 3d–f, top), which was assigned to residual water (IR spectrum of water is shown in Figure S4 in the Supporting Information). In the case of the treated cell, a weak PTIR signal is recorded at 2200 cm^{-1} (Figure 3f, bottom) which was also assigned to the absorption of residual water, and at 1925 cm^{-1} and 2017 cm^{-1} (Figure 3d,e, bottom) clear PTIR signals were recorded. This is an indication that **1** has been internalized. The mappings recorded at the two bands from **1** correspond to each other, further confirming that they are due to **1**. Interestingly, the cell showed an uneven distribution of the signals at 1925 and 2017 cm^{-1}—that is, an uneven distribution of **1**, with one hot spot—that is, a spot showing an intense PTIR signal, and cold regions—that is, regions showing a weak signal or no signal. This uneven distribution within the cells is of interest. The presence of the organometallic moiety in the conjugate may favor nuclear accumulation, as evidenced for some other organometallic bioconjugates,[27–29] and thus we decided to examine nuclear localization. The nucleus was tentatively located using irradiation at 1240 cm^{-1} (antisymmetric PO_2^- vibration) and at 1650 cm^{-1} (amide I band), as high phosphate and amide content is characteristic for the nucleus.[30] A region with a strong PTIR signal at 1240 cm^{-1} and at 1650 cm^{-1} can be seen in Figure 3 for both the control and the treated cells. In the case of the treated cell, the hot spot at 1925 cm^{-1} and 2017 cm^{-1} (Figures 3d,e, bottom) is co-localized with the hot spot at 1240 cm^{-1} and 1650 cm^{-1} (Figures 3b,c, bottom), strongly suggesting nuclear localization of **1**.

PTIR can also be used for spectromicroscopy since a spectrum can be recorded at a fixed location of the AFM tip by tuning the laser frequency. This is of utmost importance for validating the mapping images and for verifying that the PTIR signals correspond to the molecule of interest and not to background noise. High-resolution mappings were recorded at the eastern region of the treated cell, in the area determined to contain the nucleus (Figure 4). The pattern of signals observed nicely match those from Figure 3. Spectra were recorded over a large frequency range (1200–2200 cm^{-1}) at spots A and B, which correspond

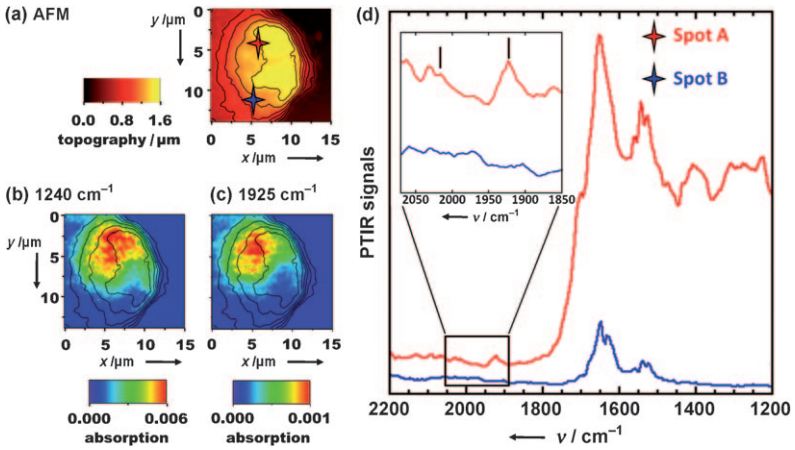

Figure 4. Enlarged image of the nucleus of the treated cell and spectromicroscopy. a) AFM topography. b,c) PTIR maps with the AFM contours superimposed as black lines recorded at 1240 cm^{-1} (b) and 1925 cm^{-1} (c). d) PTIR spectromicroscopy with an average incident power of 10 mW; spectrum at spot A in red, spectrum at spot B in blue;, inset shows the region 1850–2050 cm^{-1} region; the two ticks indicate the position of the characteristic peaks of **1**.

Received: May 25, 2010
Published online: October 12, 2010

Keywords: imaging agents · IR spectroscopy · metallocenes · spectromicroscopy · subcellular mapping

to a hot spot and a cold spot, respectively, for the signal at 1925 cm^{-1} (Figure 4d). At spot A, a spectrum clearly showing the band at 1925 cm^{-1} was recorded, whereas at spot B no such band was observed (see inset in Figure 4d). When we increased the laser power and focussed on the 1800–2200 cm^{-1} region, a spectrum clearly displaying the two expected bands at 1925 and 2017 cm^{-1} was recorded at spot A. For comparison, this spectrum is shown in Figure 2d together with FTIR spectra recorded on a collection of treated cells, control cells, and pure **1**; the positions of the IR bands in all cases match well. A spectrum in the region of the nucleus was also recorded for the control cell and no signal in the 1800–2200 cm^{-1} region was observed (see Figure S5 in the Supporting Information). These observations unambiguously indicate that the PTIR signal observed at the nucleus is due to **1**.

In conclusion, we report herein: 1) the successful detection and quantification of a metal–carbonyl compound in whole cells by classical FTIR spectroscopy and 2) the first mapping of an exogenous compound in single human cells and in the cell nucleus by PTIR spectroscopy. These experiments were performed after the cells had been incubated with a 10 µM solution of **1**. Since the IR signature of the metal–carbonyl unit was used, the organometallic derivative did not require any further tagging that might modify its physicochemical properties and hence its location. Moreover, PTIR spectroscopy was used to localize the nucleus without the use of any nucleus tracker. This is of utmost interest as PTIR is a noninvasive technique that can be applied directly to single cells. Thanks to this technique, nanometer resolution is now attainable for label-free imaging using IR radiation, and subcellular IR imaging is possible. More generally, the development of metal–carbonyl IR probes may be of interest for use in tagging other molecules for PTIR imaging, as they are small stable units. We are currently working towards the development of such probes for PTIR experiments.

[1] P. Dumas, G. D. Sockalingum, J. Sulé-Suso, *Trends Biotechnol.* **2007**, *25*, 40–44.
[2] H. Fabian, N. A. T. Thi, M. Eiden, P. Lasch, J. Schmitt, D. Naumann, *Biochim. Biophys. Acta Biomembr.* **2006**, *1758*, 874–882.
[3] M. Salmain, A. Vessières, G. Jaouen, I. S. Butler, *Anal. Chem.* **1991**, *63*, 2323–2329.
[4] A. Vessières, S. Top, A. A. Ismail, I. S. Butler, M. Louer, G. Jaouen, *Biochemistry* **1988**, *27*, 6659–6665.
[5] N. Metzler-Nolte, *Angew. Chem.* **2001**, *113*, 1072–1076; *Angew. Chem. Int. Ed.* **2001**, *40*, 1040–1043.
[6] H. W. Peindy N'Dongo, I. Neundorf, K. Merz, U. Schatzschneider, *J. Inorg. Biochem.* **2008**, *102*, 2114–2119.
[7] G. R. Stephenson in *Bioorganometallics—Biomolecules, labeling, medecine* (Ed.: G. Jaouen), Wiley-VCH, Weinheim, **2006**, pp. 215–262.
[8] M. Salmain, A. Vessières, A. Varenne, P. Brossier, G. Jaouen, *J. Organomet. Chem.* **1999**, *589*, 92–97.
[9] M. Salmain, A. Vessières in *Bioorganometallics—Biomolecules, Labeling, Medicine*, *Vol. 1* (Ed.: G. Jaouen), Wiley-VCH, Weinheim, **2006**, pp. 263–302.
[10] K. V. Kong, W. Chew, L. H. K. Lim, W. Y. Fan, W. K. Leong, *Bioconjugate Chem.* **2007**, *18*, 1370–1374.
[11] K. Meister, J. Niesel, U. Schatzschneider, N. Metzler-Nolte, D. A. Schmidt, M. Havenith, *Angew. Chem.* **2010**, *122*, 3382–3384; *Angew. Chem. Int. Ed.* **2010**, *49*, 3310–3312.
[12] P. Hildebrandt, *Angew. Chem.* **2010**, *122*, 4642–4644; *Angew. Chem. Int. Ed.* **2010**, *49*, 4540–4541.
[13] P. Lasch, D. Naumann, *Biochim. Biophys. Acta Biomembr.* **2006**, *1758*, 814–829.
[14] M. Keilman, T. Taubner, R. Hillenbrand, F. Keilmann, *Nano Lett.* **2006**, *6*, 1307–1310.
[15] A. Dazzi in *Thermal Nanosystems and Nanomaterials* (Ed.: S. Volz), Springer, Berlin, **2009**, pp. 469–503.
[16] A. Dazzi, M. Reading, P. Rui, K. Kjoller, Patent WO/2008/143817, **2008**.
[17] To record in a broadband as tuning range, we used the CLIO free-electron laser at the IR centre in Paris-Sud 11 as a laser source. Its characteristics are given in the Supporting Information.
[18] A. Dazzi, R. Prazeres, F. Glotin, J.-M. Ortega, *Infrared Phys. Technol.* **2006**, *49*, 113–121.
[19] A. Dazzi, R. Prazeres, F. Glotin, J.-M. Ortega, M. Al-Sawaftah, M. de Frutos, *Ultramicroscopy* **2008**, *108*, 635–664.
[20] A. Dazzi, R. Prazeres, F. Glotin, J.-M. Ortega, *Ultramicroscopy* **2007**, *107*, 1194–1200.
[21] A. Dazzi, F. Glotin, R. Carminati, *J. Appl. Phys.* **2010**, *107*, 124519.
[22] The prism geometry (angle) has been desinged to have a propagative wave inside the cell and the total reflection is only at the interface with the air. This means that the cell is illuminated in its entirety. Hence, the signal recorded is the integration over the complete thickness of the cell.

[23] J. Houel, S. Sauvage, P. Boucaud, A. Dazzi, R. Prazeres, F. Glotin, J.-M. Ortega, A. Miard, A. Lemaître, *Phys. Rev. Lett.* **2007**, *99*, 217404.
[24] E. A. Hillard, A. Vessières, S. Top, P. Pigeon, K. Kowalski, M. Huché, G. Jaouen, *J. Organomet. Chem.* **2007**, *692*, 1315 – 1326.
[25] S. Top, H. El Hafa, A. Vessières, J. Quivy, J. Vaissermann, D. W. Hughes, M. J. McGlinchey, J.-P. Mornon, E. Thoreau, G. Jaouen, *J. Am. Chem. Soc.* **1995**, *117*.
[26] I. Ott, K. Schmidt, B. Kircher, P. Schumacher, T. Wiglenda, R. Gust, *J. Med. Chem.* **2005**, *48*, 622 – 629.
[27] J. B. Waern, H. H. Harris, B. Lai, Z. Cai, M. M. Harding, C. T. Dillon, *J. Biol. Inorg. Chem.* **2005**, *10*, 443 – 452.
[28] F. Noor, A. Wuestholz, R. Kinscherf, N. Metzler-Nolte, *Angew. Chem.* **2005**, *117*, 2481 – 2485; *Angew. Chem. Int. Ed.* **2005**, *44*, 2429 – 2432.
[29] I. Neundorf, J. Hoyer, K. Splith, R. Rennert, H. W. Peindy N'Dongo, U. Schatzschneider, *Chem. Commun.* **2008**, 5604 – 5606.
[30] E. Gazi, J. Dwyer, N. P. Lockyer, J. Miyan, P. Gardner, C. Hart, M. Brown, N. W. Clarke, *Biopolymers* **2005**, *77*, 18 – 30.

